frontiers | Frontiers in Earth Science

TYPE Original Research
PUBLISHED 11 January 2023
DOI 10.3389/feart.2022.990253



OPEN ACCESS

EDITED BY
Sumer Chopra,
Institute of Seismological Research, India

REVIEWED BY
Nitesh Khonde,
Birbal Sahni Institute of Palaeosciences (BSIP), India
Min Wang,
University of Texas at San Antonio, United States

*CORRESPONDENCE
Zhikun Ren,
rzk@ies.ac.cn

SPECIALTY SECTION
This article was submitted to Geohazards and Georisks, a section of the journal Frontiers in Earth Science

RECEIVED 09 July 2022
ACCEPTED 05 December 2022
PUBLISHED 11 January 2023

CITATION
Ji H, Ren Z, Zhu M, Min W, Liu J and Feng Y (2023), Identification of the late Quaternary activity of the littoral fault zone at the Northern Jiangsu province in China.
*Front. Earth Sci.* 10:990253.
doi: 10.3389/feart.2022.990253



# Identification of the late Quaternary activity of the littoral fault zone at the Northern Jiangsu province in China

Haomin Ji[1,2], Zhikun Ren[1,2]*, Menghao Zhu[1,2], Wei Min[1,2], Jinrui Liu[1,2] and Yingci Feng[3,4]

[1]State Key Laboratory of Earthquake Dynamics, Institute of Geology, China Earthquake Administration, Beijing, China, [2]Key Laboratory of Seismic and Volcanic Hazards, China Earthquake Administration, Beijing, China, [3]Key Laboratory of Ocean and Marginal Sea Geology, South China Sea Institute of Oceanology, Chinese Academy of Sciences, Guangzhou, China, [4]Innovation Academy of South China Sea Ecology and Environmental Engineering, Guangzhou, China

It has been accepted that a littoral fault zone (LFZ) exists at the Northern Jiangsu Province, but its geometric distribution and the late Quaternary activity are still controversial. In this study, to constrain its late Quaternary activity, we collected two high-resolution shallow-reflection seismic profiles crossing the northern segment of the littoral fault zone (NLFZ) in the Yellow Sea, using mini-multichannel seismograph. Four reflection interfaces were identified clearly in the reflection profiles, dividing Quaternary strata in the study area into four seismic units. Combined with the existing regional borehole data, it is inferred that these units correspond to strata in the Holocene, the Late Pleistocene, the Middle Pleistocene, and the Early Pleistocene. The breakpoints $F_1$, $F_2$, $F_3$, $F_4$, $F_5$, and $F_6$ correspond to the NLFZ, and the uppermost offset marker is the Late Pleistocene–Holocene interface. Therefore, the NLFZ is tentatively identified as a Late Pleistocene–Holocene active fault. Our method utilized to obtain high-resolution profiles also provides a good example for research studies at similar sites. Moreover, considering the regional tectonic background, its fault length, and long aseismic period, the NLFZ is capable of generating strong earthquakes of Mw 6.5 or above in the future, which needs further investigation. Finally, based on our profiles and previous studies, it is inferred that the kinematic properties of the LFZ transformed at the Middle Pleistocene, at least.

KEYWORDS

**the littoral fault zone, mini-multichannel seismic seismograph, geometric distribution, the late Quaternary activity, seismogenic potential**

## 1 Introduction

The existence of the littoral fault zone (LFZ) at Northern Jiangsu Province has long been recognized by researchers (Xu et al., 1984; Yuan, 1988; Chen et al., 1991; Hao et al.,. 2010; Gao and Wu, 2000; Zhang et al., 2007; Wang B et al., 2008; Zhang et al., 2017; Wang et al., 2020; Yang et al., 2020); however, its precise location and activity have not been

**TABLE 1** List of historical and modern earthquakes in the study area.

| Date | Magnitude | Focal depth/km | Epicentral position | Longitude/° (E) | Latitude/° (N) |
|---|---|---|---|---|---|
| 2021.11.17 | 5.0 | 17 | South Yellow Sea | 121.19 | 33.50 |
| 2013.4.21 | 5.3 | 10 | South Yellow Sea | 124.6 | 35.2 |
| 1996.11.9 | 6.1 | | South Yellow Sea | 123.1 | 31.83 |
| 1984.5.21 | 6.1 | 16 | South Yellow Sea | 121.66 | 32.6 |
| 1984.5.21 | 6.2 | 16 | South Yellow Sea | 121.6 | 32.64 |
| 1932.8.22 | 6.25 | | South Yellow Sea | 121.6 | 36.1 |
| 1921.12.1 | 6.5 | | South Yellow Sea | 122 | 33.7 |
| 1927.2.3 | 6.5 | | South Yellow Sea | 121 | 33.5 |
| 1910.1.8 | 6.75 | | South Yellow Sea | 122 | 35 |
| 1879.4.4 | 6.5 | | South Yellow Sea | 122.5 | 34 |
| 1853.4.23 | 6 | | South Yellow Sea | 124.6 | 32 |
| 1853.4.15 | 6 | | South Yellow Sea | 121.5 | 33 |
| 1853.4.14 | 6.5 | | South Yellow Sea | 121.5 | 33.5 |
| 1847.11.12 | 6 | | South Yellow Sea | 122 | 33 |
| 1846.8.4 | 7 | | South Yellow Sea | 122 | 33.5 |
| 1672.6.17 | 6 | | Ju County, Shandong Province | 118.8 | 35.6 |
| 1668.7.25 | 8.5 | | Tancheng County, Shandong Province | 118.5 | 34.8 |
| 1624.2.10 | 6 | | Yangzhou City | 119.4 | 32.3 |
| 1505.10.19 | 6.5 | | South Yellow Sea | 123 | 32.5 |
| 701.8.16 | 6 | | South Yellow Sea | 121 | 33 |
| 70B.C.6.1 | 7 | | Anqiu City, Shandong Province | 119.2 | 36.3 |

determined (for example, Map of Active Tectonics in China compiled in the early 21st century did not identify this fault due to lack of clear evidence (Deng, 2007)). In particular, more than 10 destructive earthquakes, including three earthquakes greater than Mw 6 and the recent Yancheng earthquake Mw 5.0 on 17 November 2021, have occurred since 1764 alone in the south Yellow Sea (Department of Earthquake Damage and Defense, CEA., 1999) (Table 1), and the distribution of these earthquakes, consistent with the trend of small earthquakes shown by the previous small earthquake relocation work (Wang et al., 2020), is mainly in the NW direction and suggests that the trend of their seismogenic fault is similar to that of the LFZ. However, studies in the south Yellow Sea have mainly concentrated on the middle and deep layers for oil and gas exploration, stratigraphic distribution, and tectonic evolution since the Mesozoic and Cenozoic (Guo et al.,. 1997; Feng et al., 2008; Hao et al., 2010; Dai, 2011; Gao and Zhou, 2014; Guo et al., 2014; Wu et al., 2015; Yang et al., 2020; Hu et al., 2022), and the research on the late Quaternary activity of active marine faults is rarely reported. Even the geometric distribution of the LFZ has been in dispute, which was only tentatively determined by locations of earthquakes and gravitational prospecting (Xu et al., 1984; Yuan, 1988; Chen et al., 1991; Hao et al.,. 2010; Gao and Wu, 2000; Zhang et al., 2007; Wang B et al., 2008; Zhang et al., 2017). Especially, due to lack of medium–strong seismic activity, many studies suggest that the LFZ should not extend northward beyond the Northern Jiangsu province–south Yellow Sea (NJSYS) Basin (Figure 1B) (Guo et al., 2013; Cui et al., 2017; Wang et al., 2020), that is, the LFZ is only an internal fault in the basin. In view of the aforementioned observation, we selected the part of the LFZ where the NJSYS basin intersects the Middle uplift (Figure 1B), which has the most intense dispute and weakest seismic activity, to carry out geometrical and kinematics research to find out its location and evaluate its late Quaternary activity and seismic potential.

In order to determine the latest activities of active marine faults, it is essential to choose a suitable geophysical exploration method to provide high-resolution profiles of Quaternary sediments in the fault zone (Deng et al., 2002). Despite the recent advances in sub-surface imaging, making it possible to

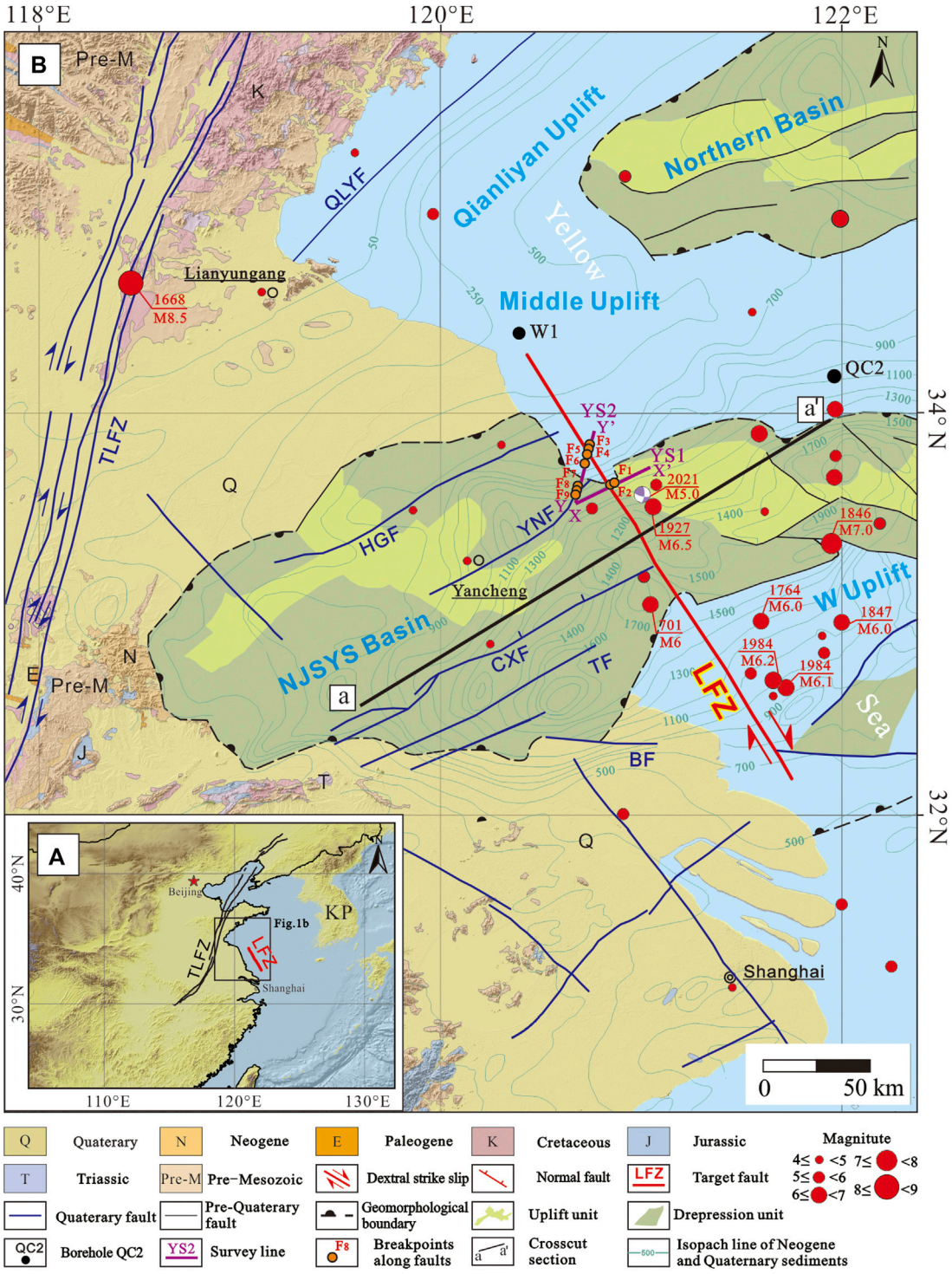


FIGURE 1
**(A)** Map showing the overall tectonic setting around the LFZ. KP: Korean Peninsula; LFZ: the littoral fault zone at the Northern Jiangsu Province; TLFZ: the Tanlu fault zone; **(B)** geological and geomorphic maps around the LFZ. HGF: the Hongze–Goudun Fault; CXF: the Chenjiabao–Xiaohai Fault; BF: the Bingchahe Fault; TF: the Taizhou Fault; YNF: the Yancheng–Nanyangan Fault; QLYF: the Qianliyan Fault; NJSYS Basin: the Northern Jiangsu–south Yellow Sea Basin; W Uplift: Wunansha Uplift.

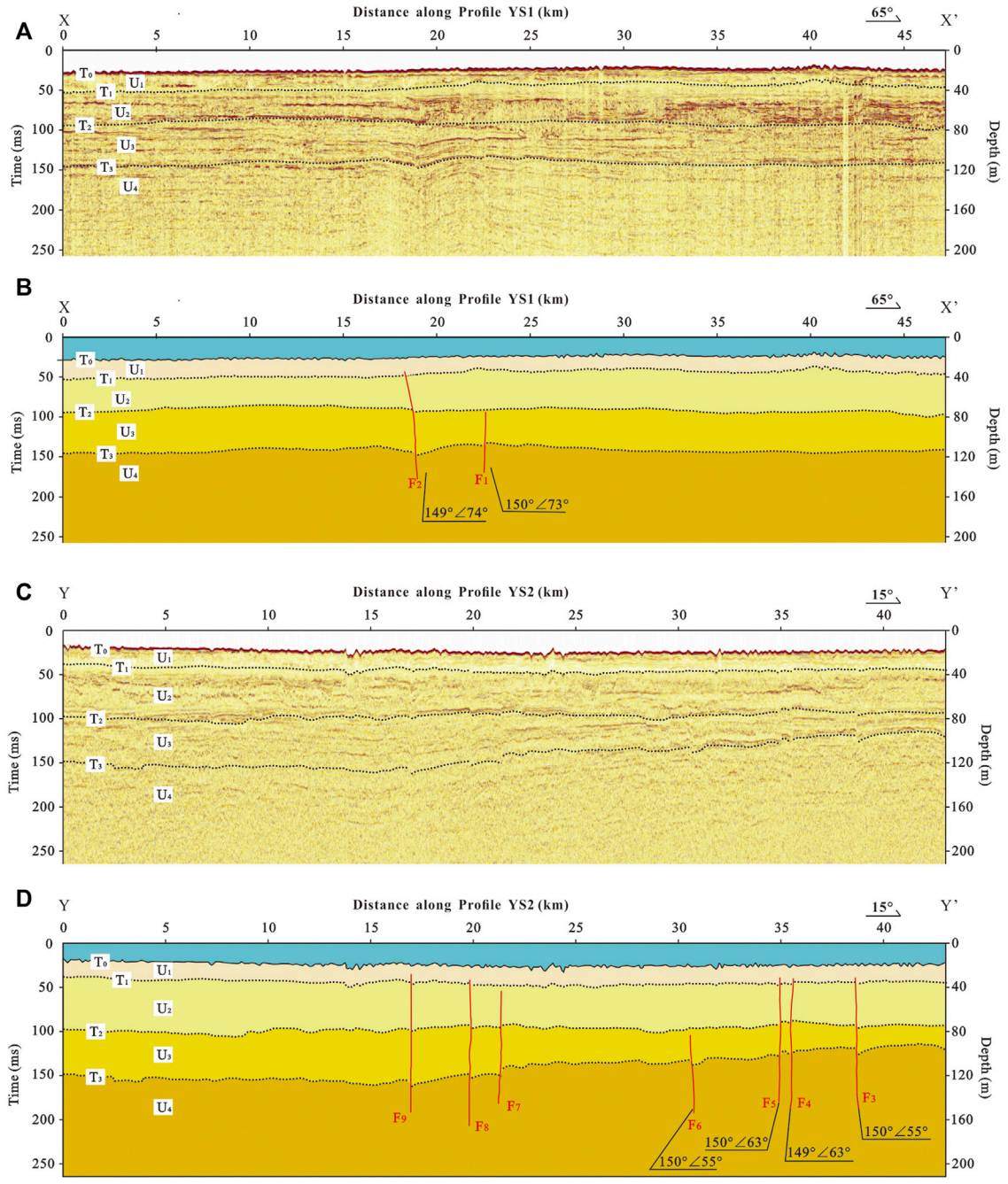


FIGURE 2
Seismic reflection profiles and interpretation results. **(A,B)**: YS1 profile; **(C,D)**: YS2 profile; $T_0$–$T_3$: seismic reflection interfaces; $U_1$–$U_4$: seismic units.

obtain high-resolution deep seismic data (Armijo, 2005; Brothers et al., 2015; Sahakian et al., 2017), the Quaternary sedimentary thickness in the Yellow Sea area is usually 20–300 m (Lin, 2017), and conventional methods find it difficult to ensure the resolution of the Quaternary sediment profiles. For example, acoustic shallow stratigraphic profiler technology (Wang B et al., 2008) and multichannel seismic exploration (Shen et al., 2013) have been carried out on the Qianliyan Fault (Figure 1B) in the Yellow Sea, but its Quaternary activity was not accurately defined due to the limit of resolution.

In this study, we used mini-multichannel seismic exploration technology to explore the northern segment of the LFZ (NLFZ)

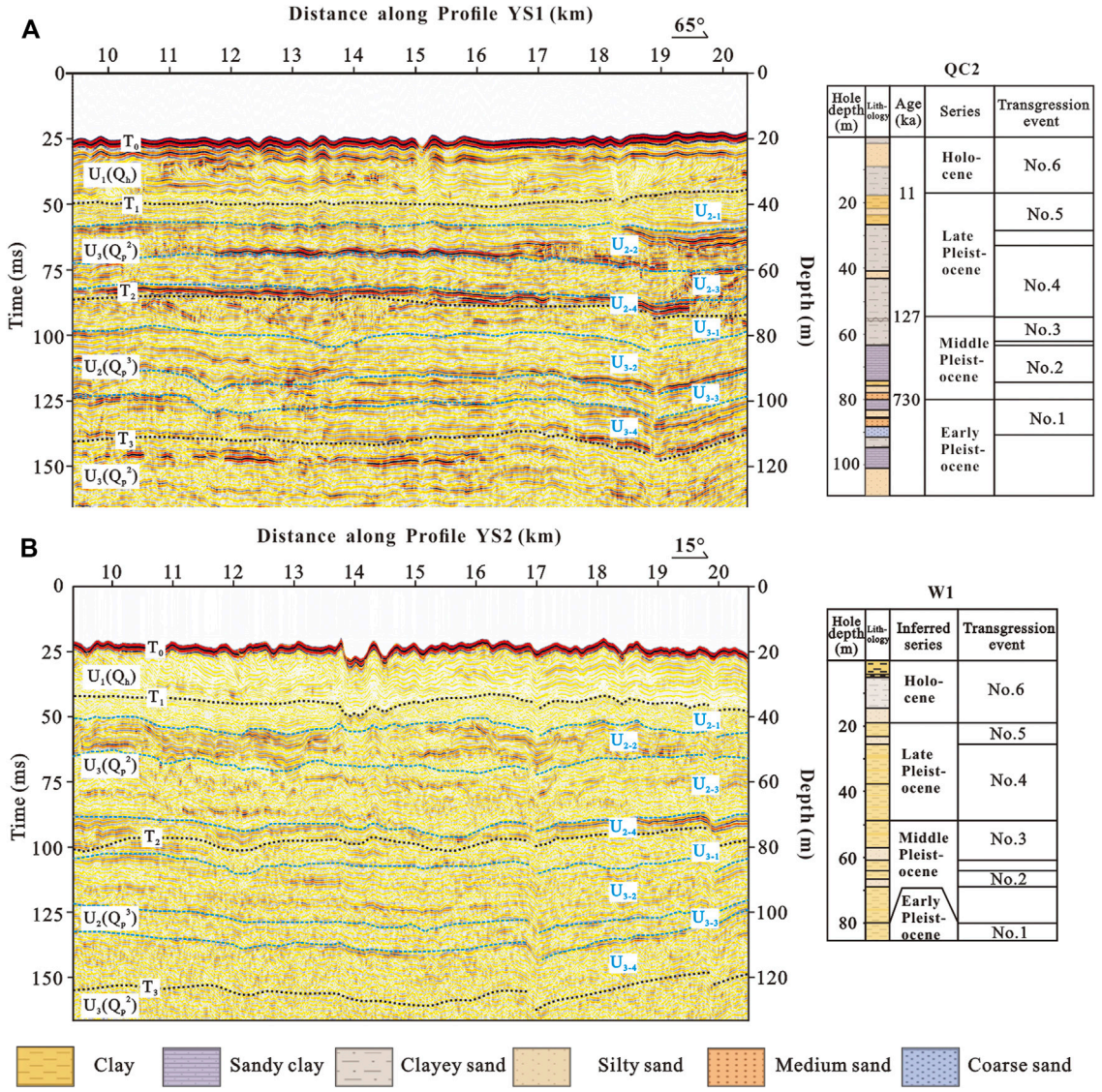


FIGURE 3
Comparison between seismic units and stratigraphic units. **(A)** comparison between YS1 and QC2; **(B)** comparison between YS2 and W1. $T_0$–$T_3$: seismic reflection interfaces; $U_1$–$U_3$, $U_{2-1}$–$U_{3-4}$: seismic units.

in an attempt to obtain high-resolution profiles and find out its geometric distribution and the latest activity and to provide an effective geophysical exploration method for active fault research in similar sites.

## 2 Geological setting

The south Yellow Sea consists of five secondary tectonic units, namely, the Qianliyan Uplift, Northern Basin, Middle Uplift, Northern Jiangsu province–South Yellow Sea (NJSYS) Basin, and Wunansha Uplift (Chen et al., 1991). According to a series of seismic reflection profiles in the south Yellow Sea region (Zheng, 1989; Chen et al., 1991; Hou et al., 2019), the uplift effect of the Middle and Wunansha uplifts only lasted until the early Cenozoic, and their uplift characteristics have become obscure since the late Neogene, and then the whole south Yellow Sea region started to receive Quaternary deposits.

Existing works, including boreholes (Supplementary Table S1), columnar core stations, and seismic reflection profiles, tentatively identified Quaternary sediment distribution and changes in the sedimentary environment in the south Yellow Sea area (Yang et al., 1984; Tao, 2009; Wan and Chen. 2016; Liu et al., 2021) (Supplementary Figure S1). Since the Early

**TABLE 2 List of recognition breakpoints in YS1 and YS2.**

| Presumed fault | No. | Seismic section | Breakpoint number | Latitude/N | Longitude/E | Apparent dip |
|---|---|---|---|---|---|---|
| Littoral fault zone | 1 | YS1 | $F_1$ | 33°39′ 17.283″ | 120°58′ 13.413″ | 42.50 |
| | 2 | YS1 | $F_2$ | 33°38′ 46.832″ | 120°57′ 0.061″ | 44.87 |
| | 3 | YS1 | $F_3$ | 33°53′ 05.222″ | 120°48′ 34.727″ | 43.84 |
| | 4 | YS2 | $F_4$ | 33°51′ 15.778″ | 120°47′ 59.501″ | 36.30 |
| | 5 | YS2 | $F_5$ | 33°50′ 57.200″ | 120°47′ 53.492″ | 45.80 |
| | 6 | YS2 | $F_6$ | 33°48′ 31.201″ | 120°47′ 6.311″ | 46.54 |
| Yancheng–Nanyangan fault | 7 | YS2 | $F_7$ | 33°43′ 30.144″ | 120°45′ 29.170″ | 37.20 |
| | 8 | YS2 | $F_8$ | 33°42′ 45.906″ | 120°45′ 14.179″ | 49.26 |
| | 9 | YS2 | $F_9$ | 33°41′ 34.151″ | 120°44′ 45.578″ | 58.31 |

Pleistocene, the south Yellow Sea shelf has experienced six large-scale transgression events (No. 1–No. 6, Supplementary Tables S1, S2) (Zheng, 1989; Wan and Chen, 2016; Liu et al., 2021). The sedimentary strata in the late Early Pleistocene were fluvial and littoral shore depositions, and then they turned into coastal shallow marine facies deposition at the end of the period because of the No. 1 transgression event. After that, the sedimentary strata in the Middle Pleistocene, which is about 30 m in thickness, were marine and continental sedimentary alternations due to two transgression events (No. 2 and 3) and showed a complex sedimentary environment (Zheng, 1989; Wan and Chen. 2016). Due to two transgression events with short intervals (No. 4 and 5), the sedimentary strata of the Late Pleistocene are mainly marine sediments with a thickness of ~30 m and local coarse deposits (Yang et al., 1984; Wan and Chen. 2016). Holocene sedimentary strata are also mainly marine sediments about 20 m thick (No. 6 transgression event) (Zheng, 1989; Wan and Chen. 2016).

The study area is mainly located in the NJSYS Basin. This basin is a Meso-Cenozoic continental basin developed on the basement of thrust nappe in the Meso-Paleozoic and is composed of late Cretaceous and Cenozoic strata (Lian et al., 2001). Since the Mesozoic, it has experienced a series of complicated tectonic deformations. From the Late Jurassic to the early Cretaceous, the thrust–nappe system was the main tectonic style in the basin (Lian et al., 2001). After that, because of the influence of Pacific plate subduction, it entered the development stage of extensional basin, including the depression basin stage in the late Cretaceous and the fault basin stage in the Paleogene (Yang and Chen, 2003). Since the Neogene, the fault basin has experienced overall subsidence and transformed into a large depression basin with the effect of the Himalayan orogeny, and then it was widely overlaid by Neogene and Quaternary strata (Liu et al., 2010).

According to their trends, the faults in the study area could be divided into two groups, Northeast (NE) and Northwest (NW) (Figure 1B). The faults trending NE, such as the Hongze–Goudun fault and the Yancheng–Nanyangan fault, controlled depressions in the Northern Jiangsu Basin, most of which are tensile faults with relatively low activity and few earthquakes (Guo et al., 2013). The southern depression of the south Yellow Sea Basin was controlled by faults trending NW (Gao and Wu, 2000), such as the LFZ, according to the locations of earthquakes (Wang B et al., 2008; Wang et al., 2020), and these faults may be the major seismogenic structures in this region with strong activity.

The LFZ, located in the transition area from the coastal area to the northern Jiangsu land area, is a crustal fault in Eastern China that controls the development of the coastline of the Northern Jiangsu Province and is also an important boundary between the neotectonic movements and modern tectonic movements of the Northern Jiangsu Province and the south Yellow Sea (Gao and Wu, 2000); the whole fault, which is about 270 km long and mainly dextral, strikes NW and cuts through the NJSYS Basin. The evidence of the isopach lines of Neogene to Quaternary sedimentary (Lv et al., 2022, Figure 1B), seismic activity (Department of Earthquake Damage and Defense, CEA., 1999; Wang, et al., 2020), and submarine topography (Lv et al., 2022) suggest that the LFZ in the NJSYS Basin may have been intensely active since Neogene with weak activity at both ends. More than ten destructive earthquakes have occurred along the fault and its adjacent areas, among which the largest earthquake was the Mw 6.5 earthquake on 3 February 1927, and the most recent strong earthquake was the Mw 6.2 earthquake in the south Yellow Sea on 21 May 1984 (Wang B et al., 2008; Wang, et al., 2020). The LFZ may be the seismogenic fault of these earthquakes and be of high seismic activities in the late Quaternary. Recently, a moderate–strong earthquake also occurred in this region, the Yancheng Mw 5.0 earthquake on 17 November 2021 (Figure 1B), which may indicate that this region is of high seismic potential in the future.

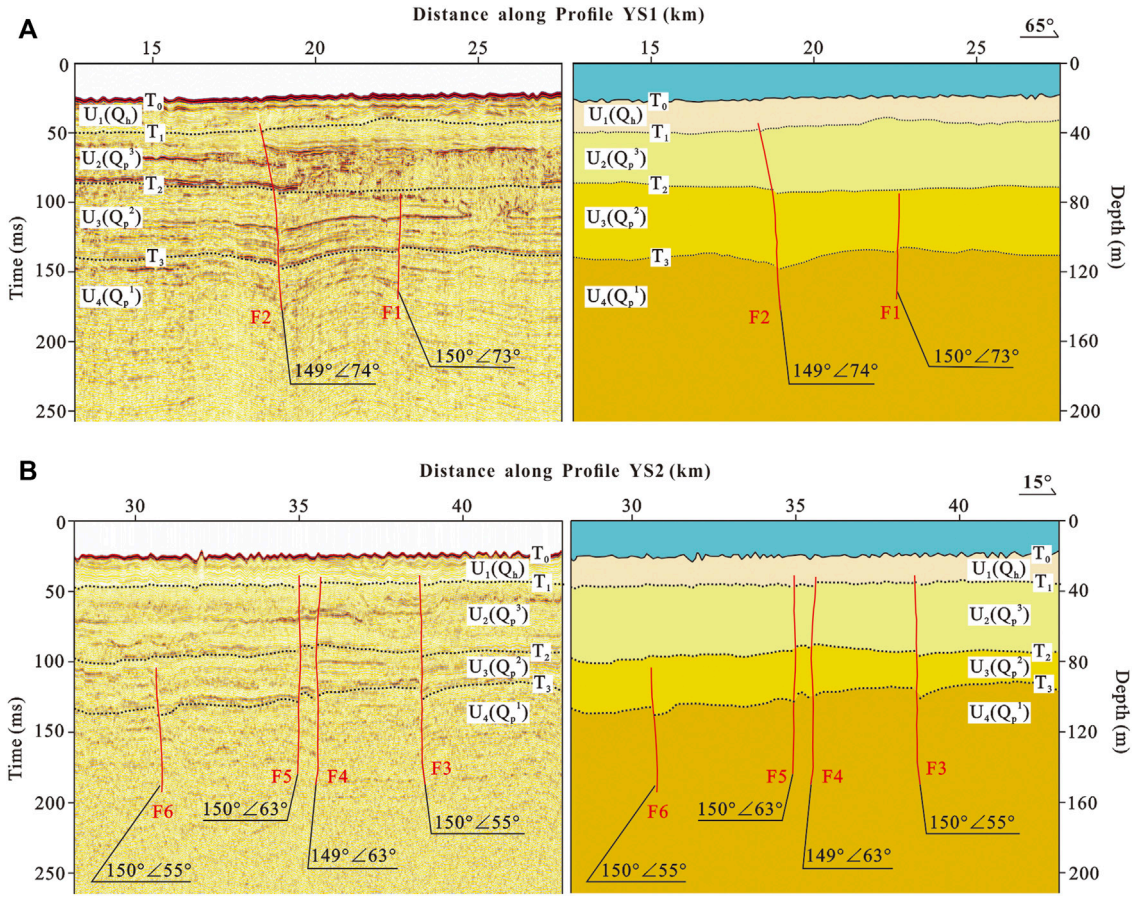


FIGURE 4
Characteristics of the interpreted faults revealed by profiles. **(A)** YS1 profile; **(B)** YS2 profile.

## 3 Method

Seismic reflection technology can be used to find out the offset location of active faults at relatively deep layers (Deng et al., 2002). Generally, seismic reflection techniques include shallow stratigraphic profile and multi-channel and single-channel seismic exploration. Shallow stratigraphic profile exploration is usually used in near-surface due to its high frequency and weak penetration ability (Didailler et al., 2002; Liu et al., 2005; Zhang et al., 2017); the single-channel seismic reflection method with a low signal-to-noise ratio is often used in depth ranges below 1 km underground (Xing, 2012); traditional multi-channel seismic detection is also suitable for deep detection because of its long array and large channel spacing (Yang and Li, 2007; Wang Z C et al., 2008; Kühn et al., 2021; Maria and Ramana, 2021). However, borehole data (Lin, 2017) show that the thickness of Quaternary sediments in the Yellow Sea is usually 20–300 m. Therefore, based on previous studies (Zhao et al., 2011; Xing, 2012; Li et al., 2020; Wu et al., 2020; Yi et al., 2022), we chose the sparker source, which has relatively good performance in revealing the characteristics of shallow fault structures, narrowed channel spacing and used mini-multichannel seismic exploration, which is characterized by high precision, high resolution, high signal-to-noise ratio (SNR), strong penetration ability, and less interference sources, to detect the NLFZ and its adjacent sea area.

In this study, according to the fault strike, two survey lines, YS1 (48 km long) and YS2 (42 km long), were designed across the fault (Figure 1B). The Geo Sparker source (800 J) with a shot interval of 1 s was utilized to generate signals, and its data allowed a vertical resolution of 30 cm. Then, the data were obtained through 24 channels in a geo-sense multichannel streamer made in Netherlands with group intervals of 3 m, 36-m-long streamer, and were recorded at 0.1 ms sampling intervals and 500 ms trace length. The data were processed through RadExpro software. Pre-stack processing of the seismic data included bandpass filtering, amplitude correction, marine geometry, velocity analysis, normal moveout corrections, and stack. Post-stack data were processed by demultiple and Kirchhoff migration (Meng et al., 2007; Xing, 2012; Pan et al., 2015; Luo et al., 2020; Yang et al., 2020).

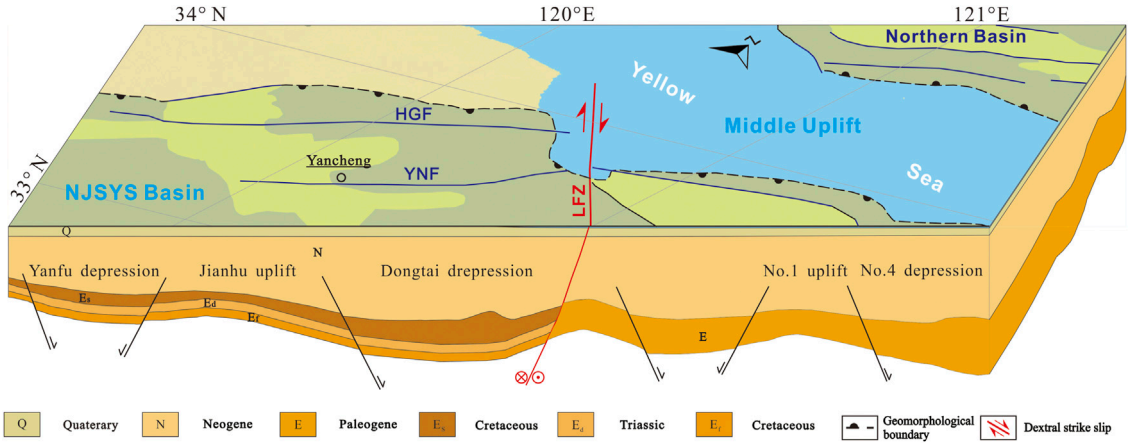


FIGURE 5
Cross-section of the littoral Fault. Geological information was taken from Yao et al., 2008 and Liu et al., 2014. See Figure 1B for the location of section a–a′.

Finally, the clear deep structures could be observed from the final profiles, which were used in the analysis of the fault activities.

# 4 Result

## 4.1 The identification of seismic reflection interfaces

The high-resolution seismic reflection profiles obtained by this study can clearly distinguish marine and continental strata (Figures 2A, C), but there is abundant shallow gas distributed in the study area, whose seismic reflection characteristics are mainly acoustic blank, that is, shielded area. The existence of shallow gas shielded the seismic signals of the lower layer and cut off the continuity of the strata, which brought some difficulties to the interpretation of the seismic data.

After the processes of filter and gain processing, we used seismic stratigraphy approaches to distinguish the contact relationships of the seismic units (Zhao, 2003) in the seismic profiles and finally identified a series of regional unconformity or pseudoconformity seismic reflection interfaces ($T_0$~$T_3$) based on continuous traceable events in both seismic reflection profiles (Figures 2A, C).

$T_0$ is the reflection interface of the seabed and is characterized by strong amplitude, high energy, and high continuity. Its undulating form reflects the seabed's topographical changes. Compared with $T_0$, $T_1$ has a little lower continuity and similarly strong amplitude, whose interface obviously fluctuates and suggests strong cut and erosion. $T_2$ is a reflection interface with medium–strong amplitude and good continuity. Its interface is relatively flat and has obvious erosion and cutting effects on the underlying strata, and the stratum structures above and below the interface are obviously different. $T_3$ has weak amplitude, high frequency, good layer continuity, and obvious fluctuation change, which can be basically tracked in the whole region, but many places along it were discontinuous due to later reconstruction.

## 4.2 Comparison between seismic units and stratigraphic units

The seismic reflection profile can only prove the existence of faults and find out the latest offset interface. In order to obtain the formation age of seismic units and infer the latest activity of faults, it is usually necessary to drill core samples and date them, but offshore drilling is difficult to carry out due to the huge cost. Fortunately, a series of works, including boreholes (Supplementary Table S1), seismic reflection profiles, and columnar core stations, have been deployed in the south Yellow Sea area to identify the Quaternary sediment distribution (Zheng, 1989; Tao, 2009; Wan and Chen, 2016; Liu et al., 2021) (Supplementary Figure S1, Supplementary Table S1). Among them, borehole QC2 had the most complete sedimentary sequence since the early Pleistocene and a high core recovery rate (90.4%), with relatively reliable formation age obtained by paleomagnetic, isotope dating, spore powder, oxygen isotope, and other methods (Yang et al., 1984) (Supplementary Table S2). In addition, QC2 revealed all large-scale regression–transgression cycles since the late Early Pleistocene (Figure 3A, Supplementary Table S2). Although QC2 is located at the Middle Uplift (34°18′N and 122°16′E, Figure 1B), there has been no large-scale tectonic activity in the south Yellow Sea region since the Neogene, and existing research studies also

indicate that the NJSYS Basin and Middle Uplift are mainly located in the Old Yellow–Huai River Delta, with an approximate sedimentary environment and sedimentary sequence since the Quaternary (Yang et al., 1984; Tao, 2009; Wan and Chen, 2016). In addition, there was an engineering borehole (Figure 1B, borehole W1) on the north side of the two seismic sections, although it does not have chronological work, based on historical record and the comparison with borehole QC2. Wan and Chen, (2016) thought W1 also revealed almost all transgression events and its sedimentary environment since the Early Pleistocene was very similar to those of QC2's (Figure 3B, Supplementary Table S3). Therefore, the borehole QC2 could be used as a reliable reference for stratigraphic division in this study.

As mentioned previously, existing research studies revealed six large-scale transgression events in the south Yellow Sea region since the late Early Pleistocene (Yang et al., 1984; Tao, 2009; Wan and Chen, 2016; Liu et al., 2021), corresponding to six sets of marine strata. Marine strata often have regular and parallel reflection structures with strong continuity and can be traced in a wide range. By contrast, the internal reflection structure of continental strata is relatively chaotic with poor continuity and small distribution (Tao, 2009). On top of that, seismic units in two sections were carefully tracked and compared based on the continuity, frequency, amplitude, internal structure characteristics, and external reflection patterns of seismic reflection wave groups; finally, they were divided into four stratigraphy units (Figures 2B, D), named U1, U2, U3, and U4 from young to old.

Unit $U_1$, located between reflection interfaces $T_0$ and $T_1$, is a marine deposit formed since the Holocene (Figures 3A, B). Due to the change of seabed topography and modern tidal movement, the acoustic reflection wave characteristics and regional distribution of this layer have had a great change in the transverse direction. Sediments in $U_1$ are generally thick in the near shore and thin in the far shore. This layer extends eastward with a continuous and clear acoustic phase and gradually coincides with the seafloor.

$U_2$ unit, widely distributed in the study area, is the Late Pleistocene sedimentary (Figures 3A, B), including two marine and continental sedimentary cycles, which can be divided from the top to the bottom:

$U_{2-1}$: Continental deposits formed during the last glacial period, which can be distinguished as paleo-channel, paleo-lake, paleo-depression, and paleo-weathering crust;

$U_{2-2}$: Marine strata formed in the Late Pleistocene, with low amplitude, low energy, and high continuity, corresponding to the No. 5 transgression event;

$U_{2-3}$: Continental deposits with disordered filling structure formed in the middle Late Pleistocene;

$U_{2-4}$: Regional marine deposits with low amplitude and high continuity formed in the early Late Pleistocene (No. 4 transgression event).

Unit $U_3$ is the Middle Pleistocene stratum (Figures 3A, B), and it can also be subdivided into the late Middle Pleistocene continental strata with chaotic seismic facies ($U_{3-1}$), late Middle Pleistocene marine strata with strong continuity, medium amplitude and large thickness ($U_{3-2}$, No.3 transgression event), middle and late Middle Pleistocene continental strata with mixed and disorderly facies ($U_{3-3}$, No. 2 transgression event), and the Middle Pleistocene marine strata with moderate amplitude and strong continuity ($U_{3-4}$).

Unit $U_4$ is the late Early Pleistocene stratum (Figures 3A, B). Due to the limited drilling depth of QC2 and W1, we only interpreted the upper part of U4, which is also the marine strata and corresponds to the No. 1 Trangression event.

### 4.3 Result of fault identification

The fault characteristics on the seismic profile are generally corresponding to those of the geological profile. Generally, the vertical offset of events of a reflection wave means the offset of the stratum; similarly, a distorted area or the reflection blank belt along the reflection wave event may suggest the fault fracture zone. According to the general identification features such as the offset, shape mutation, fork, and sudden change of the amount of the reflection wave events, we interpreted the seismic profile of this collection and identified totally nine breakpoints; detail logs are provided in Table 2. Among them, two breakpoints were identified on the YS1 line (Figure 2B) and seven on the YS2 line (Figure 2D).

The location of breakpoints is projected in Figure 1B, and the distribution of breakpoints is relatively dense. Several nearly parallel faults can be obtained by connecting breakpoints $F_1$ and $F_3$ and $F_2$ and $F_5$, respectively. These faults are within 4 km in width, dipping NE with dip angles of 55°–75° at breakpoints. These results are roughly consistent with the strike and location of the LFZ based on seabed topography, seismic activity distribution, and deep data in previous studies (Xu et al., 1984; Gao and Wu, 2000; Tian et al., 2004; Wang B et al., 2008; Li et al., 2018; Wang et al., 2020; Lv et al., 2022). Combined with the regional structure, it is considered that the faults reflected by $F_1$, $F_2$, $F_3$, $F_4$, $F_5$, $F_6$, and $F_6$ are the LFZ, which is a fault zone composed of parallel faults. Faults $F_7$, $F_8$, and $F_9$ suggest the extension of the Yancheng–Nanyangan Fault in the sea.

## 5 Discussion

### 5.1 The latest activity of the northern segment of the littoral fault zone

The fault zone revealed by seismic profiles (Figure 1B) is located in the NLFZ and the Yancheng–Nanyangan Fault (YNF). $F_1$ and $F_2$ on YS1 both dislocated the $T_2$ interface, and then $F_2$ continued to offset the younger $T_1$ interface, but waves above $F_1$ are continuous (Figure 4A); thus, $F_1$ was only active in the Late Pleistocene and $F_2$ in

the Late Pleistocene–Holocene Fault. YS2 revealed four sub-faults ($F_3$–$F_6$). $F_6$ only offsets the $T_3$ interface. Similar to $F_2$, $T_1$, $T_2$, and $T_3$ interfaces at $F_3$, $F_4$, and $F_5$ all have well-consistent vertical displacement, $U_2$ and $U_3$ units on both sides of these faults also have significant changes, and it is inferred that $F_3$, $F_4$, and $F_5$ should be the Late Pleistocene–Holocene active fault. Therefore, the NLFZ is tentatively identified as the Late Pleistocene–Holocene active fault.

Although there is no direct evidence in previous studies, a series of existing indirect evidence around the fault zone could also be used to verify the accuracy and reliability of the interpretation results in this study and promote the comprehensive study of faults.

The LFZ was first revealed by the high-precision aeromagnetic survey conducted by the Ministry of Geology and Mineral Resources in China (Cui et al., 2017), and the trend of the LFZ was inferred to be NW. In addition, the isopach lines of Neogene to Quaternary sedimentary (Lv et al., 2022) show obvious differences on both sides of the LFZ (Figure 1B). The strike of isopach lines west of the basin is mainly NE, and the sedimentary thickness is thicker, more than 1,800 m, then decreases to the east. Isopach lines of marine deposits east of the LFZ mainly strike NW, suggesting that the fault activity is significantly affected the distribution of sediments. The sea floor topography (Lv et al., 2022) also shows that there are NW-trending grooves in the NJSYS Basin, and then the topography becomes flat to the north and south, indicating that the LFZ may have been active since Neogene and its activity may be mainly concentrated in the NJSYS Basin. Last but not least, seismic activity along the LFZ and its adjacent sea area has been intense for the last 300 years, which may suggest that the LFZ is the seismogenic structure in this region with strong activity. Therefore, these indirect pieces of evidence demonstrate that the activity of the LFZ may be more in the late Quaternary, consistent with our results.

In conclusion, based on the results of the mini-multichannel seismic survey and other research studies, the NLFZ is identified as the Late Pleistocene–Holocene active fault. Our two profiles give the exact location of the NLFZ, demonstrating that the fault cuts the NJSYS Basin and continues developing northward. Our method, which was used to obtain high-resolution profiles, also proved that it can be popularized in research studies at similar sites. Since the active age of the NLFZ in this study is a conjecture based on the evolution of sedimentary environment and the existing borehole data in the south Yellow Sea, it still needs to be verified by further borehole data near the fault zone.

## 5.2 Transformation of kinematic properties of the littoral fault

Existing research studies indicate that the movement of the LFZ is mainly strike–slip with dip–slip component (Yuan et al., 1988; Chen et al., 1991; Gao and Wu, 2000). Although our sections do not reveal the strike–slip displacement of the NLFZ, we can observe relatively obvious normal dip–slip components, e.g., $F_2$, $F_3$, $F_4$, and $F_5$, vertically dislocated the nearby strata (Figure 4), and the measured vertical displacement of the NLFZ is 1.8–5.2 m from the top to the bottom. However, according to the overall stratigraphic distribution revealed by the sections (Figure 2), these strata have not been significantly affected by fault activity since the Middle Pleistocene. Based on our results, the isopach lines of Neogene to Quaternary deposits and previous research studies (Yao et al., 2008; Liu et al., 2014; Lv et al., 2022), we made a geological profile a–a' in the interior of the NJSYS Basin, perpendicular to the middle of the LFZ, whose location is shown in Figure 1B. The profile a–a' (Figure 5) shows that the sediments west of the LFZ in the Neogene gradually thickened to the east; thus, the LFZ constituted the boundary fault of the Dongtai Depression with the western normal fault of this depression and controlled the deposition in the depression in the Neogene, indicating that the normal dip–slip displacement of the LFZ in the Neogene was large; not only that, but the isopach lines around the LFZ did not show obvious dextral deformation. Therefore, the activity of the LFZ in the Neogene may mainly be normal dip–slip, which is in sharp contrast to the result that the LFZ has been mainly strike–slip since the Middle Pleistocene. We inferred that, at least since the Middle Pleistocene, the kinematic properties of the LFZ have changed from the normal dip–slip to the strike–slip, and its influences to the regional sedimentary have been also significantly reduced.

## 5.3 Seismic risk assessment of the northern segment of the littoral fault zone

Previous studies have shown (Li et al., 2007) that Quaternary sediments may cover the fault and make the traces of fault activity obscure, for example, the activity of the seismogenic faults for the Mw 7.2 Xingtai earthquake in 1966 and the Mw 7.8 Tangshan earthquakes in China. Geophysical exploration results showed that their fault up-breakpoints were terminated in Late Pleistocene sediments. Therefore, the seismic risk assessment should not only be based on the upward termination of the fault traces but also combined with the tectonic background, the seismic activity, and the current tectonic stress field.

The NLFZ and its adjacent sea area have weak modern seismicity, and no earthquake of magnitude 5 or above has occurred on this segment since the recorded history. However, our results showed that the NLFZ should be a Late Pleistocene, even Holocene active fault, suggesting that the NLFZ may correspond to a seismic gap. In addition, according to the focal mechanism solution of small earthquakes, Wang Z. C. et al., 2008 believes that the principal compressive stress axis of the source stress field in Jiangsu and the south Yellow Sea is NEE, favorable to the development of NW and NNE faults. Especially, although the evidence of isopach lines and topography indicate that the LFZ within the Wunansha Uplift has been weak in activity, its seismic activity has been intense in the past 300 years and may enter the active period. Based on the

analysis of analogy, the NLFZ may be just in the quiet period of earthquakes at present, and the possibility of future moderate and strong earthquakes cannot be excluded. Therefore, the NLFZ should be considered a major seismogenic structure of moderate or strong earthquakes in the future.

The following empirical equations for the magnitude and surface rupture length (SRL) have been established from the previous study (Wells and Coppersmith, 1994) on strike–slip faults:

$$M = a + b\log SRL \quad (1)$$

where M is the magnitude, SRL is the surface rupture length, and a and b are constant parameters.

The calculation result of future earthquakes along the NLFZ based on its length of 50 km within the Middle Uplift is about Mw 7. Considering the history of about Mw 6.5 earthquakes in the LFZ, the NLFZ is capable of generating an earthquake of Mw 6.5 in the future, which is the main seismogenic structure in the study area.

## 6 Conclusion

In this study, we deployed two profiles across the NLFZ using mini-multichannel seismograph to detect its activity. Our profiles show clear layers of Quaternary sediments and convincing evidence of fault activity. Four reflection interfaces were identified clearly, dividing the Quaternary strata in the study area into four seismic units. Combined with the existing regional borehole data, it is inferred that these units correspond to the strata in the Holocene, Late Pleistocene, Middle Pleistocene, and Early Pleistocene. The breakpoints $F_1$, $F_2$, $F_3$, $F_4$, $F_5$, and $F_6$ correspond to the NLFZ, and the uppermost offset marker is the Late Pleistocene–Holocene interface. Therefore, the NLFZ is tentatively identified as a Late Pleistocene–Holocene active fault. According to its long aseismic period and fault length, we roughly estimate that the NLFZ is capable of generating Mw 6.5 earthquakes in the future, posing a great seismic hazard threat in this region. Our method utilized to obtain high-resolution profiles also provides a good example for research studies at similar sites. In addition, based on our sections and previous studies, we infer that the kinematic properties of the LFZ transformed at the Middle Pleistocene, at least, from the normal dip–slip to the strike–slip.

## Data availability statement

The original contributions presented in the study are included in the article/Supplementary Material; further inquiries can be directed to the corresponding author.

## Author contributions

HJ wrote the draft and prepared the figures. MZ, WM, JL, and YF collected the seismic profiles together. JL also helped prepare the figures. ZR initiated the idea, analyzed the results, and wrote the manuscript.

## Funding

This study was financially supported by the National Key Research and Development Program of China [Grant Number 2017YFC1500401], the National Science and Technology Basic Resources Investigation Program of China [Grant Number 2021FY100103], and the National Natural Science Foundation of China [Grant Number 42102273].

## Acknowledgments

We are very grateful to the predecessors for the large body of work on structural characteristics and deformation. We also thank our editor Professor Sumer Chopra and two reviewers for their fruitful comments.

## Conflict of interest

The authors declare that the research was conducted in the absence of any commercial or financial relationships that could be construed as a potential conflict of interest.

## Publisher's note



## Supplementary material

The Supplementary Material for this article can be found online at: https://www.frontiersin.org/articles/10.3389/feart.2022.990253/full#supplementary-material

# References

Armijo, R. (2005). "Seismic Hazard in the Istanbul Region, Turkey–How To Study a Submarine Fault[C]," in *67th EAGE conference and exhibition*.

Brothers, D. S., Conrad, J. E., Maier, K. L., Paull, C. K., Mcgann, M., and Caress, D. W. (2015). The Palos Verdes Fault offshore Southern California: Late Pleistocene to present tectonic geomorphology, seascape evolution, and slip rate estimate based on AUV and ROV surveys. *J. Geophys. Res. Solid Earth* 120 (7), 4734–4758. doi:10.1002/2015JB011938

Chen, X., Mao, Z. Y., and Wang, F. T. (1991). The geology and seismicity of the southern Huanghai (Yellow sea) [J]. *Seismol. Geol.* (3), 205–212. (in Chinese with English abstract).

Cui, M., Zhang, G. C., Wang, P., Qi, P., and Cai, J. (2017). Characteristics and genetic mechanism of NW faults in North Jiangsu and South Yellow Sea basin[J]. *J. China Univ. Min. Technol.* 46 (6), 1332–1339. doi:10.13247/j.cnki.jcumt.000721

Dai, C. S. (2011). *Oil gas basin group of China seas and early resource assessment techniques*. Beijing: Ocean Press. ( in Chinese) [M].

Deng, Q. D., Chao, H. T., Min, W., and Zhong, Y. Z. (2002). Marine active fault exploration and Paleoearthquake research[J]. *Earthq. Res. China* 18 (3), 311–315. (in Chinese with English abstract).

Deng, Q. D. (2007). *Map of active tectonics in China [M]*. Beijing: Seismological press. ISBN:9787502830519.

Department of Earthquake Damage and Defense, CEA (1999). *Catalogue of historical strong earthquakes in China(in Chinese)[M]*. Beijing: Seismological Press.

Didailler, S., Marsset, B., Marsset, T., and Thomas, Y. (2002). Very high resolution 3D seismic: a new imaging tool for sub-bottom profiling [J]. *Comptes Rendus Geosci.* 334 (6), 403–408. doi:10.1016/s1631-0713(02)01766-2

Feng, Z. Q., Chen, C. F., Yao, Y. J., Zhang, S. Y., Hao, T. T., and Wan, R. S. (2008). Tectonic evolution and exploration target of the northern foreland basin of the South Yellow Sea[J]. *Earth Sci. Front.* 15 (6), 219–231. (in Chinese with English abstract).

Gao, S. L., and Zhou, Z. Y. (2014). Discovery of the Jurassic strata in the north-east sag of South Yellow Sea[J]. *Geol. J. China Univ.* 20 (2), 286–293. (in Chinese with English abstract). doi:10.16108/j.issn1006-7493.2014.02.013

Gao, Z. H., and Wu, S. W. (2000). Activity evaluation and tectonic significance of the Subei-Binhai Fault[J]," in *In: The eighth conference of the seismological society of China*. Changchun: Chinese Seismological Society.

Guo, B., Wang, B., and Zhang, Y. H. (2013). Seismotectonic Characteristic of Northern Jiangsu-Southern Yellow Sea Basin[J]. *North China Earthq. Sci.* 31 (1), 38–44. (in Chinese with English abstract).

Guo, X. W., Zhang, X. H., Wen, Z. H., Sun, J. W., Qi, J. H., Hou, F. H., et al. (2014). Compilation of the tectonic framework map of China seas and land and adjacent regions[J]. *Chin. J. Geophys.* 57 (12), 4005–4015. (in Chinese with English abstract). doi:10.6038/cjg20141213

Guo, Y. G., Li, Y. C., Xu, D. Y., Liu, X. Q., and Zhang, X. H. (1997). Tectonic evolution of Yellow Sea, east China sea and continental shelf and adjacent areas[J]. *Mar. Geol. Quat. Geol.* 17 (1), 1–12. (in Chinese with English abstract).

Hao, T. Y., Huang, S., Xu, Y., Mancheol, S., Liu, J. H., Dai, M. G., et al. (2010). Geophysical understandings on deep structure in Yellow Sea[J]. *Chin. J. Geophys.* 53 (6), 1315–1326. (in Chinese with English abstract). doi:10.3969/j.issn.0001-5733.2010.06.010

Hou, F. H., Guo, X. W., Wu, Z. Q., Zhu, X. Q., Zhang, X. H., Qi, J. H., et al. (2019). Research progress and discussion on formation and tectonics of South Yellow Sea [J]. *J. Jilin Univ. Earth Sci. Ed.* 49 (1), 96–105. doi:10.13278/j.cnki.jjuese.20180131

Hu, P. P., Yang, X. D., Yang, F. L., Zhang, J. C., Zhou, Z. Y., and Dong, R. W. (2022). Seismogenic Structure and Tectonic Mechanism of the 2021 Mw 5.0 Yancheng Earthquake in the South Yellow Sea Basin, East Asia. *Seismol. Res. Lett.* XX, 1–25. doi:10.1785/0220220163

Kühn, M., Karstens, J., Berndt, C., and Sebastian, F. L. (2021). Seismic reconstruction of seafloor sediment deformation during volcanic debris avalanche emplacement offshore Sakar, Papua New Guinea. *Mar. Geol.* 439, 106563. doi:10.1016/j.margeo.2021.106563

Li, C. Y., Wang, Y. P., and Wang, Z. C. (2007). Some analyses on the relation between the upper offset point and the latest activity times of buried faults in cities of eastern China. Taking the Xingtai and Tangshan earthquake regions as an example[J]. *Seismol. Geol.* 29 (2), 431–445. (in Chinese with English abstract).

Li, X. D., Liu, S. W., and Wang, L. (2018). Spatiotemporal pattern of earthquake activities and Seismotectonics in Jiangsu and Adjacent Southern Yellow Sea Area[J]. *Geol. J. China Univ.* 24 (4), 551–562. (in Chinese with English abstract). doi:10.16108/j.issn1006-7493.2018016

Li, X. J., Chen, S., Ren, Z. K., Lv, Y. J., Dong, H. Y., and Wen, Z. P. (2020). Project plan and research progress on key technologies of seismic zoning in sea areas[J]. *Prog. Earthq. Sci.* 50 (1), 2–19. (in Chinese with English abstract).

Lian, M. X., Xue, B., and Yang, S. L. (2001). Formation mechanism of depressions and rifts in the Cenozoic Basin of North Jiangsu Province[J]. *Petroleum Geol. Exp.* 23 (3), 256–260. (in Chinese with English abstract).

Lin, W. R. (2017). *The evolution of sedimentary environment and late Quaternary drilling formation of the radial sandy ridge in the southern edge of the South Yellow Sea[D]*. Nanjing: Nanjing University. (in Chinese with English abstract).

Liu, B. H., Ding, J. S., Pei, Y. L., Li, X. S., Gao, J. G., and Lv, J. F. (2005). Marine geophysical survey techniques and their applications to offshore engineering [J]. *Adv. Mar. Sci.* 23 (3), 374–384.

Liu, J., Duan, Z. Q., Mei, X., Liu, Q. S., Zhang, X. H., Guo, X. W., et al. (2021). Stratigraphic classification and sedimentary evolution of the late Neogene to Quaternary sequence on the Central Uplift of the South Yellow Sea. *Mar. Geol. Quat. Geol.* 41 (5), 25–43. (in Chinese with English abstract). doi:10.16562/j.cnki.0256-1492.2021101701

Liu, J., Saito, Y., Kong, X. H., Wang, H., Wen, C., Yang, Z. G., et al. (2010). Delta development and channel incision during marine isotope stages 3 and 2 in the Western South Yellow Sea. *Mar. Geol.* 278 (1-4), 54–76. doi:10.1016/j.margeo.2010.09.003

Liu, Y., Chen, Q. H., Hu, K., Wang, X., and Gao, F. (2014). Comparison of the Bohai Bay Basin and Subei-South Yellow Sea Basin in the Structural Characteristics and Forming Mechanism[J]. *Geotect. Metallogenia* 38 (1), 38–51. (in Chinese with English abstract). doi:10.16539/j.ddgzyckx.2014.01.008

Luo, D., Cai, F., Yan, G. J., Liang, J., Li, Q., Sun, Y. B., et al. (2020). High-resolution seismic method for shallow gas hydrates exploration[J]. *Prog. Geophsics* 36 (9), 101–108. (in Chinese with English abstract). doi:10.16028/j.1009-2722.2020.059

Lv, Y. J., Li, L. L., and Zhang, L. F. (2022). *Regional seismic safety evaluation report of Yancheng economic and technological development zone*. Unpublished.

Maria, A. D., and Ramana, M. V. (2021). Integrated analysis of magnetic, gravity and multichannel seismic reflection data along a transect southeast of Sri Lanka, Bay of Bengal: New constraints. *Mar. Geol.* 438 (2021), 106543. doi:10.1016/j.margeo.2021.106543

Meng, Q. S., Chu, X. F., Guo, X. J., Fan, Y. Q., and Jia, Y. G. (2007). The application of high resolution seismic data processing technique in multichannel shallow offshore engineering seismic surveys [J]. *Prog. Geophys.* 22 (3), 1006–1010. (in Chinese with English abstract).

Pan, J., Luan, X. W., Sun, Y. B., Zhao, T. H., Li, X. S., Liu, J., et al. (2015). The application of SRME in high resolution seismic exploration of shallow sea environment [J]. *Prog. Geophys.* 30 (1), 429–434. (in Chinese with English abstract).

Sahakian, V., Bormann, J., Driscoll, N., Harding, A., Kent, G., and Wesnousky, S. (2017). Seismic constraints on the architecture of the Newport-Inglewood/Rose Canyon fault: Implications for the length and magnitude of future earthquake ruptures. *J. Geophys. Res. Solid Earth* 122 (3), 2085–2105. doi:10.1002/2016JB013467

Shen, Z. Y., Zhou, J. P., Gao, J. Y., Wu, Z. C., Yang, C. G., Tao, C. H., et al. (2013). Quaternary faults of the Qianliyan uplift in the northern south Yellow Sea[J]. *Seismol. Geol.* 35 (1), 64–75. (in Chinese with English abstract). doi:10.3969/j.issn.0253-4967.2013.01.005

Tao, Q. Q. (2009). *The study of Paloe deltas in Western shelf of the South Yellow Sea[D]*. Qingdao: Ocean University of China. (in Chinese with English abstract).

Tian, J. M., Xu, X., Xie, H. Z., Yang, Y., and Ding, Z. (2004). Distribution characteristics of historical earthquake classes in Jiangsu Province and South Huanghai Sea Region[J]. *Acta Seismol. Sin.* 26 (4), 432–439. (in Chinese with English abstract).

Wan, P., and Chen, L. (2016). Application of paleosedimentary environment research in offshore wind power engineering investigation[J]. *Reconnaissance Sci. Technol.* 41 (1), 16–18.

Wang, B., Liang, X. P., and Zhou, J. (2008). Analysis on relationship between fault Activity and Earthquakes in Jiangsu province and its adjacent areas[J]. *Plateau Earthq. Res.* 20 (1), 38–43. (in Chinese with English abstract).

Wang, E. H., Zhang, G. W., Xie, Z. J., and Lv, Y. J. (2020). Precise relocation of small earthquakes in the Yancheng area and associated tectonic implications[J]. *Prog. Geophys.* 35 (2), 461–466. (in Chinese with English abstract).

Wang, Z. C., Chao, H. T., Du, X. S., Jia, R. G., Zhou, B., and Lu, Z. L. (2008). Preliminary study on the activity of the Qianliyan fault in the northern South Yellow Sea[J]. *Seismol. Geol.* 30 (1), 176–186. (in Chinese with English abstract).

Wells, D. L., and Coppersmith, K. J. (1994). New Empirical Relationships among Magnitude, Rupture Length, Rupture Width, Rupture Area, and Surface Displacement[J]. *Bull. Seismol. Soc. Am.* 84 (4), 974–1002. doi:10.1007/BF00808290

Wu, D. C., Zhu, X. Q., Wang, Q. L., and Hou, F. H. (2020). Characteristics of active faults related to deep faults in the northwestern part of the South Yellow Sea [J]. *Mar. Geol. Front.* 36 (2), 12–18. (in Chinese with English abstract). doi:10.16028/j.1009-2722.2019.039

Wu, Z. Q., Hao, T. Y., Zhang, X. H., Liu, L. H., Xiao, G. L., and Wen, Z. H. (2015). Contact relationships between the North China block and the Yangtze block: New constraints from upper/lower-source and long spread multi-channel seismic profiles[J]. *Chin. J. Geophys.* 58 (5), 1692–1705. ( in Chinese). doi:10.6038/cjg20150520

Xing, L. (2012). *Study of the key technologies of high-precision marine multichannel seismic survey[D]*. Qingdao: Ocean University of China. (in Chinese with English abstract).

Xu, B., Li, X. T., Wang, D. M., Luo, G. Y., Guo, Z. Y., and Guo, P. X. (1984). Regional crustal stability evaluation of southern Jiangsu Nuclear Power Station[J]. *Hydrogeology Eng. Geol.* 9 (6), 1–4.

Yang, J. J., Pan, J., Luan, X. W., Yan, Z. H., and Liu, H. (2020). Application of attenuation technology to shallow water multiples in multi-channel seismic data processing. *Mar. Geol. Quat. Geol.* 40 (1), 167–174. (in Chinese with English abstract). doi:10.16562/j.cnki.0256-1492.2018101202

Yang, Q., and Chen, H. Y. (2003). Tectonic evolution of the North Jiangsu-South Yellow Sea Basin[J]. *Petroleum Geol. Exp.* 25 (1), 562–565. (in Chinese with English abstract).

Yang, W. D., and Liu, W. J. (2007). Marine high-resolution seismic techniques applying in the geological exploration of shallow strata [J]. *Offshore oil.* 27 (2), 18–25. (in Chinese with English abstract).

Yao, Y. J., Feng, Z. Q., Hao, T. T., Xu, H., Li, X. J., and Wan, R. S. (2008). A new understanding of the structural layers in the South Yellow Sea Basin and their hydrocarbon-bearing characteristics[J]. *Earth Sci. Front.* 15 (6), 232–240. (in Chinese with English abstract).

Yi, H., Zhan, W. H., Min, W., Wu, X. C., Li, J., Feng, Y. C., et al. (2022). A comparative study of source effect based on mini-multichannel seismic profile in marine active fault detection [J]. *Seismol. Geol.* 44 (2), 333–348. (in Chinese with English abstract). doi:10.3969/j.issn.0253-4967.2022.02.004

Yuan, Y. R. (1988). Active faults in the southwest of the South Yellow Sea[J]. *Mar. Sci.* (2), 8–12.

Zhang, M. H., Xu, D. S., and Chen, J. W. (2007). Geological structure of the Yellow Sea Area from regional gravity and magnetic interpretation. *Appl. Geophys.* 4 (2), 75–83. doi:10.1007/s11770-007-0011-1

Zhang, X. J., Zhang, W., Fan, Z. L., Zhu, W. P., Tong, J., and Yao, G. T. (2017). Characteristics of airborne gravity field and the main geological discovery in the northern South Yellow Sea[J]. *Geol. Surv. China* 4 (1), 50–56. (in Chinese with English abstract). doi:10.19388/j.zgdzdc.2017.01.08

Zhao, C. B., Liu, B. J., and Ji, J. F. (2011). The acquisition technique of high-resolution seismic data for prospecting of active faults[J]. *Technol. Earthq. Disaster Prev.* 6 (1), 18–25. (in Chinese with English abstract).

Zhao, Y. X. (2003). *Quaternary seismic stratigraphic interpretation of high-resolution seismic profiles of the South Yellow Sea[D]*. Qingdao: Ocean University of China. (in Chinese with English abstract).

Zheng, G. Y. (1989). *Quaternary stratigraphy correlation in the South Yellow Sea [M]*. Beijing: Science Press. (in Chinese).